DUST ON MARS FROM NAVCAM AND HAZCAM IMAGES ON MSL

Hao Chen-Chen , **Santiago Pérez-Hoyos**, **Agustín Sánchez-Lavega**, *Departamento de Física Aplicada I, ETS Ingeniería UPV/EHU, Bilbao, Spain (hao.chen@ehu.eus)*

Introduction: Although not designed for this specific purpose, images taken by the Mars Science Laboratory (MSL) Engineering Cameras can be used for retrieving the dust optical depth and aerosols physical properties at Gale Crater (Moores *et al.*, 2015). Dust size distribution and particle shapes can be constrained by evaluating the sky brightness as a function of the scattering angle obtained from the MSL cameras (Smith and Wolff, 2014). This abstract is a progress report on our analysis of these data.

MSL Engineering Cameras: The MSL Curiosity rover is equipped with 12 engineering cameras which are built under the same design as the Mars Exploration Rovers (MER) (Maki *et al.*, 2003).

The objective of these cameras is to support the surface operations of the rover by providing views of the near-field surrounding terrain; detect, monitor and avoid hazards and to characterize the rover position and orientation; as well as supporting the operation of the robotic arm and the material sample delivery (Maki *et al.* 2012).

Navcam. The MSL Curiosity Navigation cameras consist of four-cameras mounted on the mast of the rover and have a 45-degree square field of view with a broadband response span of 600-850 nm.

Hazcam. The Hazard Avoidance Cameras (Hazcam) are rover chassis-mounted tactical cameras in the front and the rear of the vehicle with a 124-degree square FOV. They have also a broadband coverage from 600 to 800 nm.

Complete technical specifications of the imagers on MSL can be found in Maki *et al.* (2012) while information on the performance of the optics is shown in Maki *et al.* (2003).

Line-of-sight extinction: Deriving the optical depth between the rover and the crater rim provides the possibility of estimating the amount of dust airborne (Lemmon *et al.*, 2015). The line-of-sight extinction in Gale Crater as seen by the MSL Curiosity Navcam has been previously reported by other authors (Moores *et al.*, 2015, Moore *et al.*, 2016).

Following the analysis methodology by Moore *et al* (2016), a subset of Curiosity rover's Navcam observations was evaluated. All images have a size of 1024x512 pixels and were pointing North around local noon time.

The images contain the near ground around the rover, the north Gale Crater rim and the sky above. In order to calculate the line-of-sight optical depth, the spectral radiance value at these areas (ground, rim, sky) are extracted and evaluated as in Moores *et al.* (2015) at different sampling points (see Figure 1).

We have reproduced the process followed on Moore *et al.* (2016) to calculate the atmospheric extinction and we have extended the data analysis timeframe up to Sol 1292 (L_s 120º in MY33). The results obtained for the line-of-sight extinction for the five regions are presented in Figure 2. Our values match to those obtained by previous works, showing the same trend for each year and representing the variation of the line-of-sight extinction with the season. (Lemmon *et al.*, 2015)

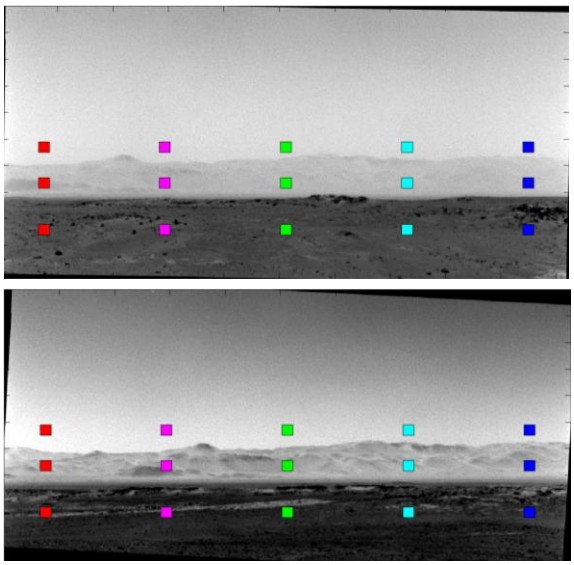

Figure 1. Example of MSL Navcam northern pointing images, corresponding to Sol 352 (L_S 0º, top) and Sol 648 (L_S 140º, bottom). Coloured squares indicate to the sampling regions at 3 different levels (ground, mountain, sky) for 5 directions, namely 'NW' (red), 'NNW' (pink), 'N' (green), 'NNE' (cyan) and 'NE' (blue).

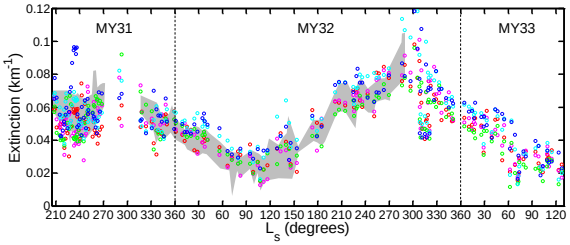

Figure 2. Line-of-sight extinction for MY31, MY32 and MY33 for the five sampling regions and comparison with envelope of results by Moore *et al.* (2016) (grey area).

Sky radiance: The brightness of the sky as a function of the scattering angle provides useful information for constraining the shape and size distri-

bution of aerosols in the atmosphere. Navcam and Hazcam images were used to determine the scattering properties of the dust.

The Navcam 'sky 360' surveys cover a wide range of angles from the sun as they were designed to determine scattering properties of the atmosphere (see Figure 3).

In addition to these images, this work has also evaluated the wide field (120 degrees) images provided by the Hazcams (see Figure 4).

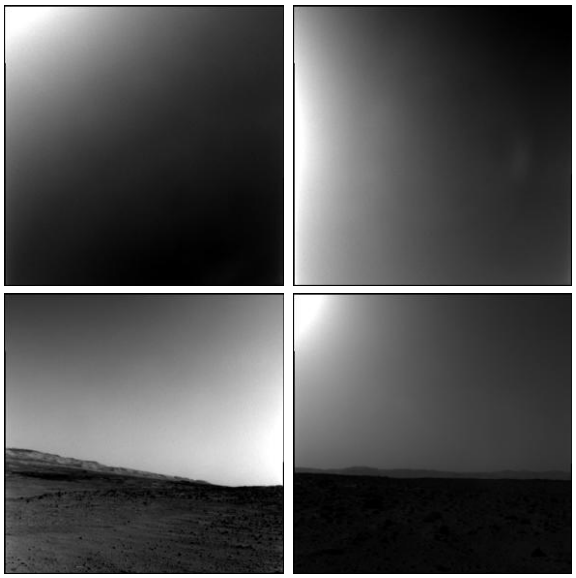

Figure 3. Example of MSL Navcam 360 sky survey sequence images for Sol 669.

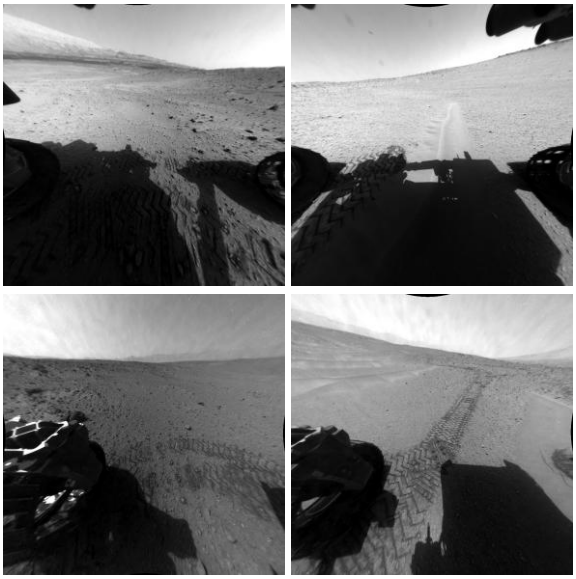

Figure 4. MSL Hazcam images for the same day (Sol 669) obtained by the cameras located at the front (top) and rear (bottom) of the rover.

Once the scattering phase function has been obtained (see Figure 5), the information on the dust particle size and shape can be estimated by computing phase functions with different models for dust to see which one reproduces the retrieval the best (Smith and Wolff, 2014). Currently, we are setting up a radiative transfer model based on DISORT (Stamnes et *al.*, 1988) in order to reproduce the observed data. An inversion algorithm based on Levenberg-Marquardt minimization of cost function is also being developed.

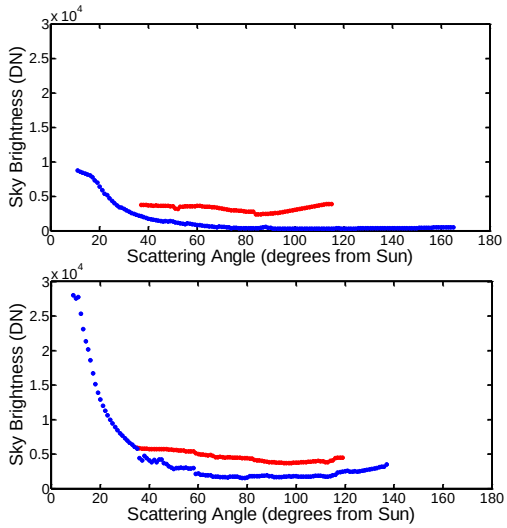

Figure 5. Comparison of sky brightness survey taken by MSL Navcam (green) and Hazcam (blue) for Sol 610 (top) and 669 (bottom).

Summary: We show that characterization of the dust on Mars can be retrieved using the Engineering Cameras on board the Mars Science Laboratory rover. The methodology provided on Moore *et al.* (2016) has been followed for obtaining the line-of-sight extinction at Gale Crater. The sky radiance has been obtained using Navcam sky survey images and Hazcam pictures and it is currently being analysed to determine dust properties as particle size and shape.

Acknowledgements: This work is supported by the project AYA2015-65041-P with FEDER support, Grupos Gobierno Vasco IT-765-13, Universidad del País Vasco UPV/EHU programme UFI11/55, and Diputación Foral Bizkaia – Aula EspaZio Gela.

References:

Lemmon, M.T., *et al.* (2015). *Icarus*, **251**, 96-111, doi:10.1016/j.icarus.2014.03.029.

Maki, J.N., *et al.*,(2003). *J. Geophys. Res.*, **108** (E12), 8071, doi:10.1029/2003JE002077.

Maki, J.N., *et al.* (2012). *Space Sci. Rev.*, **170**, 77-93, doi:10.1007/s11214-012-9882-4.

Moore, C.A., *et al.* (2016). *Icarus*, **264**, 102-108, doi:10.1016/j.icarus.2015.09.001.

Moores, J.E., *et al.* (2015). *Icarus*, **249**, 129-142, doi:10.1016/j.icarus.2014.09.020.

Smith, M.D., and M.J. Wolff (2014). 5th MAMO, Abstract #2101.

Stamnes, K., *et al.* (1988). *App. Opt.*, **27**, 2502-2509, doi:10.1364/AO.27.002502.